Transient Vibration of a Laser Scanner Motor in Digital Electrophotography

Hiroyuki Kawamoto
Department of Mechanical Engineering, Waseda University
3-4-1, Okubo, Shinjyuku, Tokyo 165-8555, Japan
kawa@mn.waseda.ac.jp

Abstract

This paper describes a transient vibration during start-stop operation of a polygonal mirror scanner motor in a laser printer. Two types of abnormal vibration take place in the rotor driven by a flat-type brushless DC motor and supported by a passive thrust magnetic bearing and a radial air bearing. One is an axial displacement and vibration and another is a radial dry-contact at very low speed region. From results of theoretical and experimental investigations, the following characteristics and countermeasures have been deduced: (1) Repulsive magnetic force induced between the stator coils and rotor magnet of the motor causes the axial static displacement and the axial transient vibration. Soft start-stop scheme of the motor current is effective to reduce the axial vibration. (2) The rotor is statically unstable in the radial direction at very low speed region. This instability occurs because the stiffness of the air bearing is not induced without rotation and it is small at the very low speed region, whereas the magnetic negative stiffness of the magnetic bearing is existent even at a zero speed. Dry contact between the rotor and the stator shaft at the air bearing is induced at the speed lower than a threshold. Since the dry contact reduces the lifetime of the air bearing, it is preferable to avoid frequent start-stop operations and to keep the rotor speed higher than the threshold. The instability is reduced to adopt the magnetic bearing composed of a pair of permanent magnets.

Introduction

A polygonal mirror scanner motor is used in the exposure subsystem of the digital electrophotography to scan laser beam and to write latent images on the photoreceptor.[1,2] The rotation of the mirror is required to be (1) stable, constant velocity, and low vibration, to realize high image quality; (2) high speed rotation for high print speed and high resolution machines; (3) long life; (4) small heat loss; (5) low acoustic noise; and (6) low cost. The motor shown in Fig. 1 and Fig. 2 is under development to meet these requirements. The rotor is driven by a flat-type brushless and coreless DC motor. The motor consists of a ring-shape rotor made of 8-pole permanent magnet and six coreless stator coils. The stator coils, which consist of three pairs of U, V, and W-phase coils, are star-connected. The polygonal mirror is attached to the rotor. The rotor is supported in the radial direction by an outer-rotor-type self-acting grooved journal air bearing[3-8] and in the axial direction by an axially stable passive magnetic bearing.[9,10] The magnetic bearing utilizes an axial restoring magnetic force between radially magnetized rotor and stator magnets made of plastic magnet.
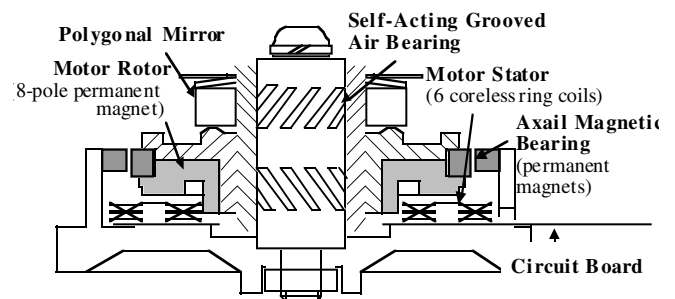

Figure 1. Configuration of polygonal mirror scanner rotor driven by flat-type brushless DC motor and supported by thrust magnetic bearing and radial air bearing.
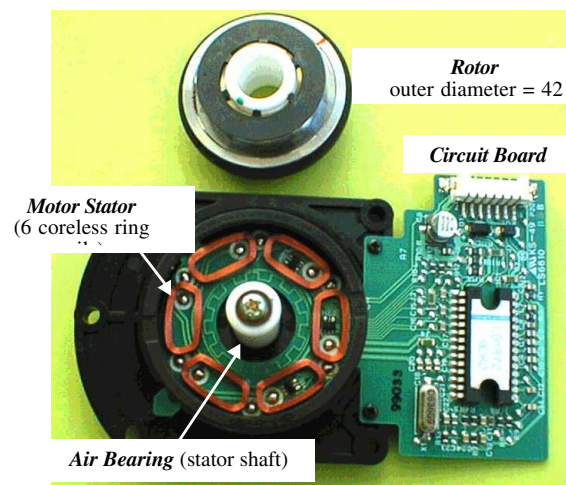

Figure 2. Polygonal mirror scanner motor. The rotor (upper) is disassembled from the stator (lower).

　　Two types of abnormal transient vibration take place in this rotor system during the startup and free-run operations. One is an axial displacement and vibration at the start-stop operation and another is radial dry-contact at very low speed region. The former prolongs the startup time and in the worst case the rotor collides with a casing. The mechanism of this vibration has been clarified and some countermeasures have been proposed.[11] On the other hand, the later is due to a static instability of the bearing system at very low speed region. This instability occurs because the stiffness of the self-acting air bearing is not induced without rotation and it is small at the very low speed region, whereas the magnetic negative stiffness of the magnetic bearing is existent in the radial direction even at zero speed. Dry contact between the rotor and shaft is induced at the speed lower than the threshold. It causes a wear of the air bearing or abrasion fragments are accidentally caught in the bearing gap. These reduce a lifetime of the scanner motor. The objectives of the present investigation are to clarify qualitative characteristics of the dry-contact and to propose an evaluation method and effective countermeasures in order to realize highly reliable digital copy machines and laser printers.

Axial Displacement and Vibration

Figure 3 shows a typical axial vibration response and motor current during start-up operation. These are measured using the motor shown in Fig. 1 with the same procedure reported in Reference 11. Since the author has already reported analytical and experimental investigations on the mechanism and methods to reduce the static displacement and vibration at the start-stop operation.[11] These are summarized in the following.
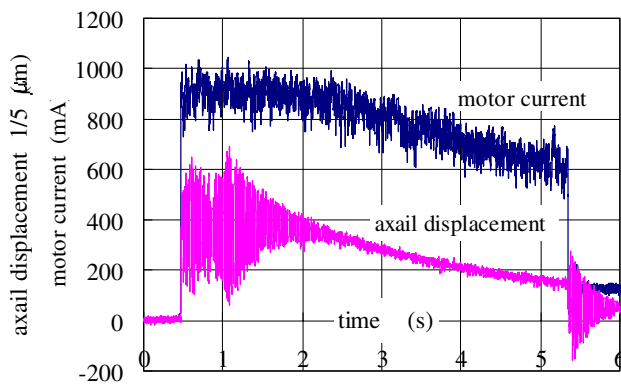

Figure 3. Measured transient vibration during start-up operation. Rated speed = 340 Hz.

Mechanism and Characteristics of Vibration

　　Magnetic force is induced between the stator coils and the rotor magnet of the flat-type DC motor under current passage. The axial force is repulsive and its magnitude is proportional to the current. The force causes the axial static displacement and the axial transient vibration is induced at

the start of operation, because a large lumped axial force is induced at this moment. The frequency of the transient vibration is a little higher than of the natural frequency at no current passage, because the frequency of the vibration at the startup operation is determined by not only the stiffness of the thrust magnetic bearing but also that of the motor. When the speed falls in the rated speed, the motor current is reduced and therefore the axial repulsive force is also reduced. The static displacement is recovered almost to the stationary position, because the repulsive force is very small under the constant speed operation. On the contrary, the axial transient vibration is induced again due to the lumped change of the repulsive force. The frequency of the vibration is determined virtually only by the axial stiffness of the thrust magnetic bearing. A large hunting of the current is sometimes observed just before and after the rotor speed fell in the rated speed and this induces large transient vibration.

Methods to Reduce Static Displacement and Vibration

　　Numerical investigation deduced that; (1) higher stiffness of the magnetic bearing and lower acceleration current linearly reduce both the static displacement and the transient vibration, however, the former may reduce a lifetime of the air bearing due to the strong dry-contact at the start and stop operation as discussed in the following chapter and the latter prolongs the startup time; (2) the transient vibration converges rapidly with high axial damping. However, the static displacement and a peak of the vibration are not reduced substantially unless the large damping close to the critical one is applied; (3) a soft start-stop scheme of the motor current is effective to reduce the vibration but it does not reduce the static displacement. The hunting current must be suppressed or, at least, coincidence of the hunting frequency and the natural frequency of the system must be avoided.

Radial Dry-Contact

Modeling on Static Instability

　　The threshold speed of the dry contact is determined as a balance of the moment applied to the rotor. It is defined as the speed under which the rotor is statically unstable and the ring (rotor) of the air bearing is in contact with the bearing shaft (stator). The speed is calculated from the condition that a natural frequency, an eigenvalue of a characteristic equation, corresponding to the axi-symmetric and rigid rotor model shown in Fig. 4 must be zero.[12] Here, the damping and non-orthogonal effect of the journal air bearing are neglected, because the natural frequency is slightly influenced by these factors.[12-15] A gyroscopic effect is also neglected, for the threshold speed is very low.

$$KK_\theta = K_{r\theta}^2 , \tag{1}$$

where $K = k + \Delta k \left| L_1 - L_2 \right|$, $K_\theta = k l^2 + \dfrac{1}{3} \Delta k \left| L_1^3 - L_2^3 \right|$,

$$K_{r\theta} = k l + \dfrac{1}{2} \Delta k \left| L_1^2 - L_2^2 \right| ,$$

k is the negative radial stiffness of the magnetic bearing, Δk is the radial stiffness per unit length of the air bearing, L_1 and L_2 are the distances form the gravitational center of the rotor to the upper and the lower end of the air bearing, and l is the distance from the gravitational center of the rotor to the magnetic bearing. The distances are defined to be positive in the upper and negative in the lower direction. The stiffness of the magnetic bearing k is constant with respect to the rotational speed but Δk is a function of the speed.
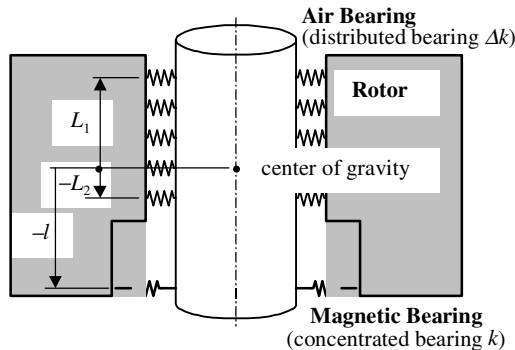

Figure 4. Vibration model. The rigid rotor is vertically supported by the 'distributed' air bearing and the 'concentrated' magnetic bearing.12

Calculation of Bearing Stiffness and Threshold Speed

The mass conservation law in a bearing gap derives the Reynolds equation. Based on the perturbation and a Divergence Formulation-Finite Element Method, the stiffness of the grooved gas bearing is numerically calculated.[16] Figure 5 shows the calculated result. It is evident that the stiffness is zero without rotation and it becomes large at high speed.
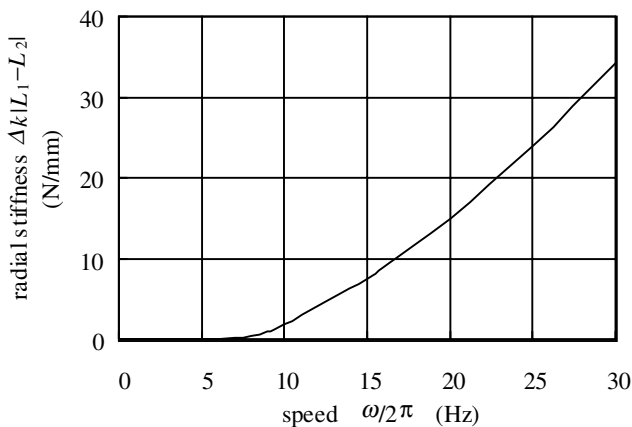

Figure 5. Calculated stiffness of air bearing. bearing width =19 mm, diameter = 11 mm, gap = 5 μm, number of groove = 11, depth of groove = 5 μm, width of groove = 1.57 mm, angle between groove and axis = 59 deg, width of non-groove area = 9.08 mm.

A direct measurement of the radial unstable stiffness of the magnetic bearing is difficult but it is indirectly estimated to be 6.7 N/mm because the measured axial stable stiffness was 2.9 N/mm and the ratio of stable and unstable stiffness of the magnetic bearing composed of a pair of ring magnets is 0.43.[*1] The threshold speed is explicitly calculated to be 15 Hz by substituting k, Δk, and the geometry into Eq. (1).

Experimental Procedure

Figure 6 shows an experimental setup to measure the axial vibration and the change of torque during start and stop operations. A black-and-white mark is painted on the top of the rotor and a pulse wave of laser beam reflection was measured by a laser displacement meter. The signals were digitized and sent to a computer where data were numerically transformed to the speed.
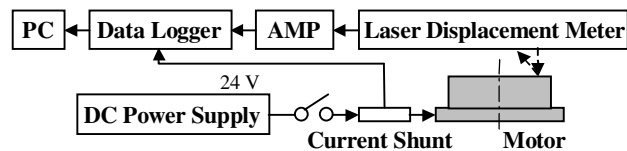

Figure 6. Experimental setup.

Results of Experiments

Figure 7 shows an axial free vibration at zero speed. Because the rotor was in contact with the stator, the free vibration was not an exponential but arithmetical decay.[*2] The measured frequency of the vibration was 43.7 Hz, which corresponded to the 2.9 N/mm axial stiffness of the magnetic bearing. This dynamically derived stiffness coincided with the statically measured value.[*3] A friction force was 0.021 N which was derived from the arithmetical decay.

Figure 8 shows a slowdown of the speed during the free-run operation. A careful observation allows us to recognize that an inflection point existed at about 15 Hz and the rate of the speed decrease was high at the speed less than 15 Hz. It can be assumed that the rotor contacted with the stator and the dry-friction decelerated the rotor speed. This assumption is clearly confirmed from Fig. 9 and Fig. 10. Figure 9 is the total mechanical loss calculated from Fig. 8.[*4] If the mechanical loss solely due to the air drag, it must be proportional to the square of the speed. The measured loss actually coincided with the curve of secondary degree at the speed higher than 15 Hz but it is larger than the curve at less than 15 Hz. The difference between the measured loss and the curve of secondary degree may due to the dry friction. Here, the curve was fitted to the secondary degree by the least square method using data at the speed higher than 16 Hz. The measured threshold speed, 15 Hz, coincided just with the numerically predicted speed, 15 Hz. Figure 10 shows the friction force derived from the difference of the loss.[*5] The friction force extrapolated at zero speed was about 0.03 N which coincided fairly well with

the force 0.021 N derived from the free vibration curve at zero speed (Fig. 7). Two independently measured forces were consistent with each other.
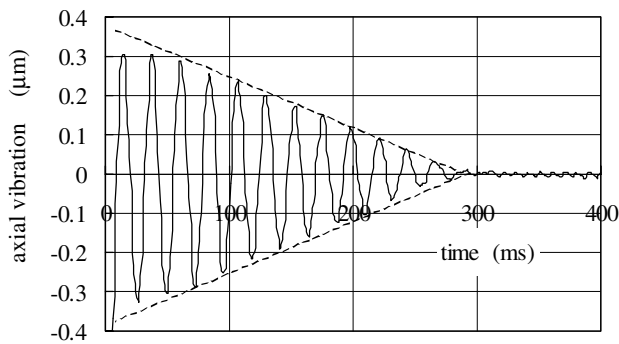

Figure 7. Axial free vibration at zero speed.
($\omega_n/2\pi$ = 43.7 Hz, friction force = 0.021 N)
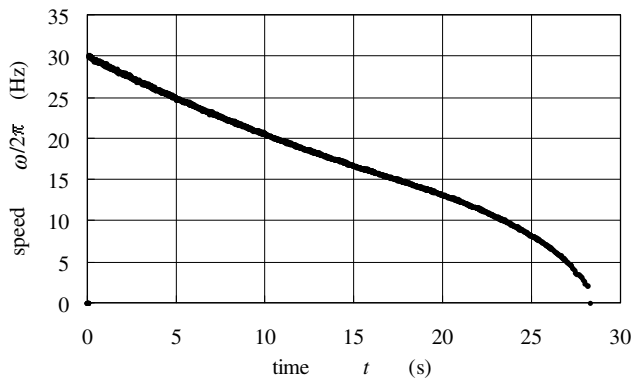

Figure 8. Slowdown of speed during free-run operation.
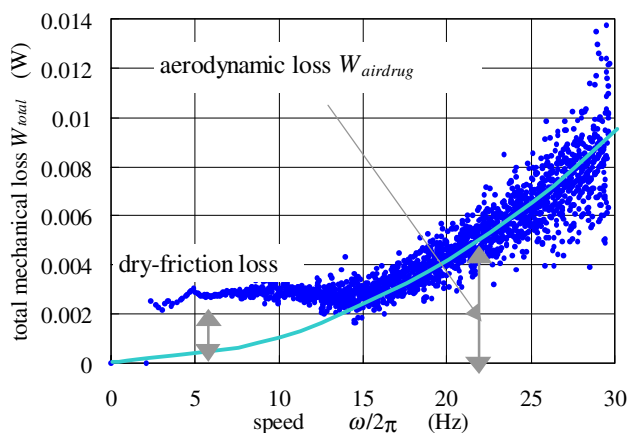
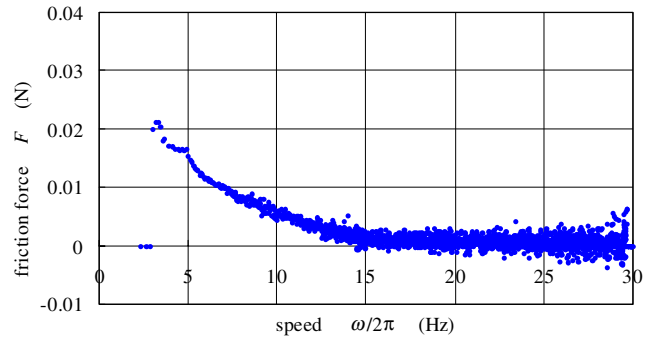

Figure 9. Mechanical loss during free-run operation.

Figure 10. Dry-friction force during free-run operation.

The evidence of the dry friction during the startup operation could not observed, because the rate of the speed increase was extremely fast (68 Hz/s) to measure the small change of the torque. The radial abnormal whirling vibration due to the dry friction was also not observed, because the radial gap of the air bearing was only 5 µm and no substantial vibration took place in the radial direction.

*1 A theoretical investigation deduces that the ratio is exactly 1/2 and it is independent of the geometry if a magnetic permeability of the permanent magnet is equal to that of the free space but it is less than $2/\pi^2$ (= 0.2) and it varies with the geometry if infinitely permeable material is used for pole yokes.[10] The measured ratio was about 0.43 for several sizes of ring magnets made of ferrite magnet. This is probably because the relative permeability of the permanent magnet is not exactly 1.0 but about 1.1−1.2.

*2 It is well known that the free vibration shows the exponential decay form with the viscous damping but it is arithmetical with the dry friction.

*3 The static stiffness was derived dividing weights put on the rotor by the static displacement measured by the laser displacement meter.

*4 The mechanical loss of the rotor is equal to $-I_p \omega \, (d\omega/dt)$, where I_p is the polar moment of inertia, ω is the rotational angular velocity, and t is time.

*5 The friction force F is $(W_{total} - W_{airdrug})/(\omega r_0)$, where W_{total} is the total loss during free-run, $W_{airdrug}$ is the loss due to the air drug, and r_0 is the radius of the air bearing.

Discussion

The following methods are effective to reduce the threshold speed and the friction force.

(1) The stiffness of the air bearing must be designed as high as possible especially in low speed region. The numerical method, Divergence Formulation-Finite Element Method,[16] is useful for the rational design.

(2) On the other hand, the radial unstable stiffness of the magnetic bearing must be designed as low as possible. This is inconsistent with realizing the high axial stiffness that is necessary to suppress the axial displacement and vibration at the start-stop operation.[11] The magnetic bearing using a

pair of permanent magnets is better than that using a steel yoke to minimize the unstable/stable stiffness ratio.[10]

(3) A static magnetic unbalance of the magnetic bearing must be minimized. Non-uniform magnetization causes the magnetic unbalance, which makes the radial displacement of the rotor and thus the large unbalance results in the large contact force. The static unbalance is estimated to be 15 μm in the present case, for the friction coefficient is 0.3, the stable/unstable stiffness ratio is 0.43, the friction force is 0.03 N at zero speed, and the axial stiffness of the magnetic bearing is 2.9 N/mm. This magnetic unbalance is larger than the mechanical unbalance, usually less than 1 μm.[14] Magnetically uniform magnet must be used and/or a magnetic balancing must be conducted.[10] The magnetic balancing is a procedure to minimize a difference between the magnetic center and the bearing center.

(4) An idling speed must be set higher than the threshold, if the motor is not stopped but driven at the low speed during the idling period.

Concluding Remarks

Analytical and experimental investigation have been performed on the radial dry-contact at the low speed region of the polygonal mirror scanner supported by the passive thrust magnetic bearing and the radial air bearing. From results of investigation, the mechanism and characteristics of the dry contact have been deduced and some countermeasures to suppress the contact force have been proposed.

The present method to measure the threshold speed of the contact will be applied to evaluate the reliability against, for example, an external excitation and a horizontal support of the rotor.

Acknowledgment

References

1. E. M. Williams, The Physics and Technology of Xerographic Processes, Krieger Publishing, Florida, 1993.
2. J. M. Fleischer, M. R. Latta and M. E. Rabedeau, *IBM J. Research and Development,* **21**, 1977, pg.479.
3. S. P. Sarraf, *SPIE* Vol. **1079**, Hard Copy Output, 1989, pg. 443.
4. J. H. Vohr and C. Y. Chow, *Trans. ASME D*, **87**, 1965, pg. 568.
5. K. Ono, A. Iwama, M. Suzuki, T. Iwamura, Y. Itami and T. Hwang, *J. Trans. of the Japan Soc. of Mechanical Engineers C,* **60**, 1996, pg.2670.
6. T. Y. Hwang, K. Ono and Y. Itami, *Proc. of Int. Conf. on Micromechatronics for Information and Precision Equipment (MIPE'97),* The Japan Soc. of Mechanical Engineers, Tokyo, 1997, pg.607.
7. S. B. Malanoski, *Trans. ASME F*, **89**, 1967, pg.433.
8. R. E. Cunningham, D. P. Fleming and W. J. Anderson, *Trans. ASME F*, **91**, 1969, pg.52.
9. H. Kawamoto, *Bulletin of the Japan Soc. of Mechanical Engineers,* **26**, 1983, pg.1654.
10. H. Kawamoto, "Magnetic Bearing for High Speed Rotors," Dr. thesis, Tokyo Institute of Technology, 1983.
11. H. Kawamoto, *J. Imaging Sci. Technol*, **43**, 1999, pg.484.
12. H. Kawamoto, *J. Imaging Sci. Technol*, **41**, 1997, pg.565.
13. A. Tondl, Some Problems of Rotor Dynamics, *Czechoslovak Academy of Sciences*, Prague, 1965.
14. R. Gasch and H. Pfutzner, *Rotordynamik-eine Einfuhrung*, Springer-Verlag, Berlin, 1975.
15. V. V. Bolotin, *Nekonservativnyie zadachi Teorii Uprugoi Ustoichivosti, Fizmatgiz,* Moscow, 1962.
16. C. Chen, N. Kawabata and M. Tachibana, *J. of Trans. of Japan Soc. of Mechanical Engineers C*, **63**, 1996, pg.2093.

Biography

Kawamoto, Hiroyuki holds a BS degree in Electrical Engineering from Hiroshima Univ. (1972) and a Dr. degree in Mechanical Engineering from Tokyo Institute of Technology (1983). From 1972 to 1991 he was a Senior Engineer at the Nuclear Division of Hitachi Ltd. In 1991 he joined Fuji Xerox, and was engaged in the research of electrophotography as a Research Fellow. In 1999 he left Fuji Xerox and he is now a professor of Waseda Univ. He was selected a Fellow of the IS&T in 1999.